Clockwise hysteresis of diatoms in response to nutrient dynamics during eutrophication and recovery

Manuela Milan [1,2] **Nina Albrecht,**[1] **Frank Peeters** [1] **Simone Wengrat** [1] **Martin Wessels,**[3]
Dietmar Straile [1]*

[1]Limnological Institute, University of Konstanz, Constance, Germany
[2]Institute for Mummy Studies, Eurac Research, Bolzano, Italy
[3]Institut für Seenforschung, LUBW, Germany

Abstract

Many lake ecosystems that have been severely disturbed by eutrophication, have also experienced large human efforts to restore "natural" conditions. However, the trajectories and the extent of recovery of these lake ecosystems are still poorly understood. In many shallow lakes, recovery was often delayed and counter-clockwise hysteretic. Here, we study recovery and ecosystem trajectories in a large and deep lake using diatom remains in sediment cores and time series of phosphorus concentrations. We identified four periods of diatom community change: slow change during early eutrophication, thereafter a short period of rapid change after the 1950s, followed by community stability from the 1960s to the mid-1980s, and finally a recovery phase until 2010. Diatom community structure responded quickly and in a saturating way to increasing phosphorus concentrations, but also fast to phosphorus decline. Hence, diatom community dynamics did not show counter-clockwise hysteresis but was characterized by a high degree of recovery and clock-wise hysteresis (CWH). We suggest that CWH in response to eutrophication and recovery is a typical and previously overlooked feature of deep lakes, which results from a more rapid change of average nutrient concentrations and thus productivity in the epilimnion compared to average nutrient concentrations across the entire water column. Such nonlinear and hysteretic responses to changing nutrients need to be considered when analyzing the effects of other stressors such as climate warming on ecosystem dynamics to prevent erroneous attribution of ecosystem change to other stressors instead of nutrient change.

Human impact on ecosystems has substantially increased in the 2nd half of the last century. This global increase in impact applies to various ecosystem stressors such as overexploitation of fish stocks, construction of large dams, and fertilizer consumption (Steffen et al. 2015). In lakes, increasing nutrient pollution, that is, eutrophication, resulted in manifold secondary consequences (Schindler and Vallentyne 2008) such as the spread of anoxic conditions (Jenny et al. 2016), and increases of harmful cyanobacteria (Taranu et al. 2015).

*Correspondence: dietmar.straile@uni-konstanz.de

Author Contribution Statement: M.W. took and dated the sediment core, N.A. and M.M. sampled the sediment core and identified diatom frustules, N.A., M.M. and D.S run the statistical analyses. M.M. and D.S wrote a first version of the paper. All authors made substantial contributions to the interpretation of the data, contributed critically to subsequent versions, and gave final approval for publication.

Hence, eutrophication severely impedes ecosystem services such as recreation and drinking water supply and causes large costs for society. For example, costs of eutrophication have been estimated to reach annually $2.2 billion in the United States and $0.1–0.16 billion in English and Welsh freshwaters (Pretty et al. 2003; Dodds et al. 2009).

Reversing the effects of eutrophication has been a major goal of environmental policy, and at least in many European and North American lakes phosphorus concentrations have been successfully reduced (Jeppesen et al. 2005). Unfortunately, ecosystem and food web responses to these concentration reductions were often delayed (Jeppesen et al. 2005). The responses of lake ecosystems have been classified into three categories (Carpenter et al. 1999): (1) irreversible, if the ecosystem is not able to return to its pre-eutrophication state, despite a reduction in P input; (2) reversible, if the ecosystem rapidly and completely restores by the sole reduction in P input; and (3) hysteretic, if the ecosystem has two alternative ecological states that are connected by different trajectories during eutrophication and recovery, respectively.

Hysteresis in the dynamics of the shallow lake ecosystems has been well studied and results from a variety of positive feedback mechanisms within a phytoplankton-dominated turbid state on one side, and within a macrophyte dominated clear state on the other side (Scheffer et al. 1993; Ibelings et al. 2007). In these shallow lake ecosystems, positive feedback results in slow system response to both nutrient enrichment and recovery, that is, counter-clockwise hysteresis (counter-CWH). Likewise, in medium deep lakes in which eutrophication did result in hypolimnetic anoxia, phosphorus release from the sediments during nutrient reduction will also cause delayed ecosystem responses during recovery (Carpenter et al. 1999).

Here, we propose CWH as a novel 4th category of system response to eutrophication and recovery typical for deep lakes without anoxic hypolimnion. In deep lakes, total phosphorus concentration measured during the late winter mixing period (TP_{MIX}) is typically used as indicator of trophic status (Salmaso et al. 2007; Thomas and Eckmann 2007; Jochimsen et al. 2013; Berthon et al. 2014; Dove and Chapra 2015). TP_{MIX} measures the total amount of phosphorus in the water column at the start of the growing season and thus provides an indication of the phosphorus stores available for primary productivity over the subsequent season (Jassby 1998; Dove and Chapra 2015). However, during eutrophication significant amounts of phosphorus will enter the lake during the vegetation period suggesting that TP_{MIX} will underestimate phosphorus availability during the subsequent growing season. This inflow is expected to result in relatively fast changes in epilimnetic phosphorus relative to TP_{MIX}, respectively, whole water column phosphorus concentrations, as the latter are buffered by the large volume of the hypolimnion in deep lakes. Likewise, epilimnetic phosphorus concentrations during recovery should also decrease fast relative to changes in TP_{MIX} as the operation of sewage plants strongly reduces phosphorus inflow into the epilimnion during the vegetation period. Hence, we expect that epilimnetic phosphorus concentrations and consequently biotic responses show CWH relative to TP_{MIX} during eutrophication and recovery.

However, not only changes in nutrient inflow but also the occurrence of additional drivers such as climate warming might influence ecosystem recovery trajectories. Such additional drivers may have shifted ecosystems to a novel state. Hence, nutrient reduction might not result in a return to the status prior to eutrophication, to the original baseline, but to a new state, a changed baseline (Duarte et al. 2009; Battarbee et al. 2012). Likewise, additional drivers might affect ecosystem trajectories during eutrophication and recovery resulting in a response pattern that may be erroneously interpreted as hysteretic dynamics with respect to trophic change, that is, pseudo-hysteretic dynamics. Vice versa, if CWH is real and not recognized, differences between eutrophication and recovery trajectories, might be erroneously attributed to a 2nd driver. Hence, in case of different trajectories between eutrophication and recovery, it might be difficult to distinguish statistically between true hysteresis, that is, ecosystem responses to increases and decreases of only one stressor, and pseudo-hysteretic dynamics caused by an additional driver shifting the dynamics during the recovery period.

Many lakes worldwide have experienced accelerated nutrient enrichment since the mid-20th century due to intensive agriculture in the catchments and industrial waste and domestic sewage entering the lakes (Carpenter and Cottingham 1997; Schindler and Vallentyne 2008). Unfortunately, most monitoring programs started after the onset of enrichment, therefore there is rarely sufficient monitoring data to compare eutrophication vs. recovery trajectories (Bennion and Simpson 2011). Instead, paleolimnological approaches represent a tool to cope with this shortcoming as they allow the reconstruction of past lake structure and function (Dubois et al. 2018; Tolotti et al. 2018) and identification of lake responses to increasing and decreasing nutrient inputs (Bennion et al. 2011). Diatoms have a high sensitivity to changes in key environmental variables, such as nutrients, temperature, pH and salinity (Bennion et al. 2004), and diatom remains are well preserved in sediments allowing reconstruction of past diatom community structure (Battarbee et al. 2001; Tolotti et al. 2018). Hence, comparing diatom community dynamics reconstructed from fossil diatoms, which record epilimnetic conditions, with time series of total phosphorus concentrations measured across the whole water column will allow to investigate the community response to trophic change and test for patterns of hysteresis.

Here, we use the diatom community composition recorded in the sediment of Lake Constance, a model system for deep perialpine lakes, to test for CWH in response to trophic change. Lake Constance has experienced profound eutrophication from the 1950s towards the 1980s, but thereafter its phosphorus concentrations have declined due to nutrient management in the catchment and have recovered to the levels of the 1950s (Jochimsen et al. 2013; Güde and Straile 2016). This combination of a strong eutrophication signal combined with marked reduction in total phosphorus concentrations to those of the 1950s makes this lake especially suited for the study of ecosystem hysteresis in deep lakes. Furthermore, the dynamics of other stressors, for example, climate change (Straile et al. 2003), which might result in changing baselines and trajectories are well known. Here, we test the following hypothesis: (1) diatom community structure in recent years differs from the one observed in the 1950s; (2) the trajectories of diatom community change do not differ between lake eutrophication and recovery; (3) in case there are differences between trajectories, they are caused by warming, that is, the observed pattern is pseudo-hysteretic.

Materials and methods

Study site

Upper Lake Constance is a warm-monomictic lake located north of the Alps between Germany, Austria, and Switzerland.

It has a surface area of 536 km^2, a volume of 48 km^3 and a maximum depth of 251 m. Its main inlet is the Alpine Rhine River, which drains an area of 6119 km^2 and contributes 61.8% of the total water inflow (Wessels et al. 1999). Lake Constance has been studied since the 1920s and continuous, seasonally resolved data are available for several decades. Lake-wide measurements of dissolved phosphorus in all tributaries revealed an inflow of > 1100 tons per year from 1967/1968 (1st survey) until the late 1970s (Güde et al. 1998). The establishment of sewage plants in the catchment from 1966 onwards and the ban of phosphate in detergents in 1980 resulted in a decline of dissolved phosphorus toward 620 tons per years in 1985/1986 and between 100 and 200 tons per year in 1995/1996 and 1996/1997 (Bührer et al. 2000). Phosphorus concentrations have been measured bi-weekly to monthly at the center of Upper Lake Constance (Wessels et al. 1999; Jochimsen et al. 2013). The longest time series is available for total phosphorus concentrations during winter mixing (February/March, TP$_{MIX}$) (Güde et al. 1998). Year-round measurements of TP in the upper 20 m of the water column are available from 1967 onwards and were used to calculate summer (July, August, September) epilimnetic TP averages (TP$_{JAS}$). Annual mean air temperatures (AT) measured at the weather station of Bregenz located at the eastern shore of the lake were acquired from the HISTALP data set (Auer et al. 2007). The diatom community of Lake Constance has been analyzed in previous paleolimnological studies using diatom frustules (Wessels et al. 1999) and DNA remains of diatoms (Ibrahim et al. 2021). However, these studies do not provide detailed analyses of diatom trajectories in respect to hysteresis.

Sediment coring and dating

Two sediment cores BO10/79 and BO10/81 (lengths ~ 55 cm) were collected with a gravity Multi-Corer from the Friedrichshafen bay, (47°37′N, 9°29′E, Wessels et al. 1999) at a depth of 149 m in May 2010. Both cores were split horizontally and one half of each core was used for visual dating. The sediment was sliced at 1 cm intervals, combined according to layer depth, and was used for different analyses, including diatoms identification and counting. Since the sediment cores were finely laminated, it was possible to date the cores visually using distinct marker beds (Fig. 1a) from large flood events which were derived from runoff data of the Alpine Rhine River (Wessels et al. 1995). This method was confirmed by radiometric dating using ^{210}Pb and ^{137}CS with other cores from nearby (Bollhöfer et al. 1994). Age estimation of individual samples was done using linear interpolation between marker beds (i.e., 1908, 1922, 1927, 1954, 1971/1972, 1987, 2005) and the sediment surface (2010). A comparison between marker bed interpolation and varve counting suggests a maximum dating error of ± 3 yr (Wessels et al. 1995).

Diatom analyses

Diatoms were prepared according to standard methods described in Wessels et al. (1999): around 1 cm^3 of wet sediment was suspended with 50 mL of H$_2$O$_2$ (30%) for one night. Then, the samples were heated at 80°C until the end of the reaction and subsequently were boiled with 5 mL of HCl (10%) until the suspension became clear. Samples were finally washed, centrifuged, and filled in 50 mL MilliQ-water. The cleaned samples were placed on a slide and fixed permanently with Naphrax® resin. For each slide 400 valves were counted at 1000× magnification under a light microscope (Zeiss Axioskop 40). Diatoms were identified at the lowest possible taxonomic level using standard literature (Krammer and Lange-Bertalot 1986), as well as recent and specific literature (Håkansson 2002; Schmidt et al. 2004; Houk et al. 2010).
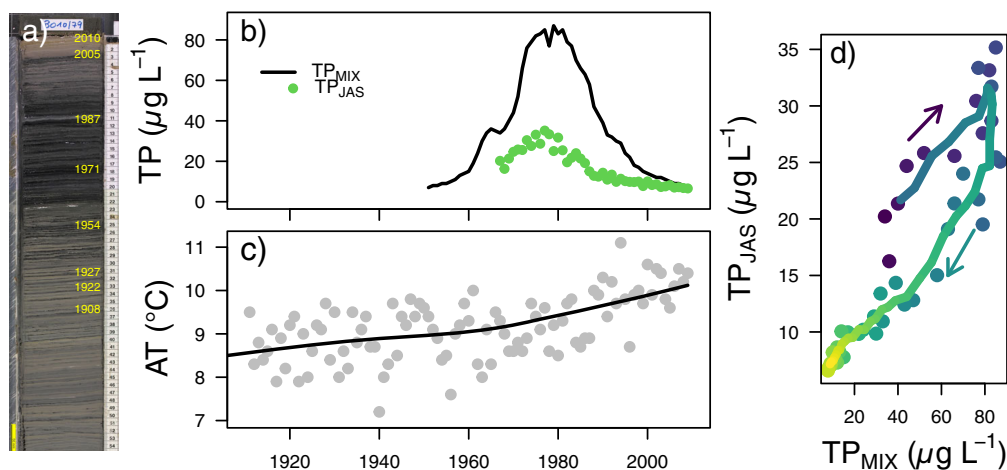

Fig. 1. Photograph of the Lake Constance sediment core and dynamics of environmental drivers. **(a)** Sediment core photograph showing distinct layers resulting from flooding events, **(b)** dynamics of TP$_{MIX}$ and epilimnetic summer TP (TP$_{JAS}$), **(c)** dynamics of AT measured at the eastern part of the lake, **(d)** relationship between TP$_{JAS}$ and TP$_{MIX}$ from the 1967 to 2010. The line in **(d)** shows a 5-yr moving average. Arrows and colors indicate the temporal development (from dark purple [1967] toward yellow [2010]).

Data analysis

For statistical analyses only diatom taxa with relative abundance values exceeding 0.5% in at least one sample were used. This resulted in a data set of 66 out of 148 diatom taxa which contributed on average 98.4% to the total diatom content in each sample. Cluster analyses and principal component analyses (PCA) were performed based on dissimilarity indices with Hellinger transformed relative abundance data (Legendre and Gallagher 2001). We run two types of cluster analyses: Depth-constrained clustering was performed to identify the timing of major shifts in the diatom community, whereas average-linkage clustering was used to analyze whether most recent years were still separated from oligotrophic periods prior to eutrophication. A broken stick model identified four significant time zones during the study period for both types of cluster analyses.

PCA results were visualized with biplots in which species scores are scaled by PCA eigenvalues. Relationships between PCA axes and the environmental variables (TP_{MIX}, AT, and year) were examined using the R function envfit. Significance of environmental variables was assessed using a permutation test ($n = 999$) (Oksanen et al. 2018). The temporal dynamics of the PCA1 scores were analyzed with segmented regression (Muggeo 2008). Performance of segmented regression models with up to 3 breakpoints was compared with Akaike's information criterion corrected for small sample sizes (AICc) and the model with the lowest AICc was chosen (Burnham and Anderson 1998).

The presence of different trajectories, that is, TP_{MIX} responses of PCA axes during eutrophication and oligotrophication and of their causes were examined using generalized additive models (GAMs) for the period 1954–2010, that is, the period when TP_{MIX} values are available. For analyses, TP_{MIX} was $\log_{10}$ transformed. Axis dynamics might not show any differences between eutrophication and recovery, that is, in models with TP_{MIX} as a predictor no residual patterns in the GAMs should be detected. Alternatively, differences between eutrophication and oligotrophication trajectories, that is, temporal patterns of residuals, might be explained via hysteresis and/or AT. Hysteresis was modeled either as a categorical variable ("period") distinguishing the eutrophication (up to 1979) and recovery (since 1980) years, or via fitting separate smooth functions of TP_{MIX} for both periods [period + s(TP_{MIX}, by "period")]. To distinguish between hypotheses, we run 8 GAMs for each PCA axis with the following predictors or GAM smooths of predictors [s(predictor)]:

m1: s(T_{PMIX}), that is, axes scores are a smooth function of TP_{MIX} (eutrophication and recovery trajectories do not differ).

m2: s(TP_{MIX}) + period, that is, axes scores are a smooth function of TP_{MIX}, but trajectories during eutrophication and recovery periods differ by a constant value.

m3: s(TP_{MIX}) + AT, that is, axes scores are a smooth function of TP_{MIX} and AT caused different trajectories.

m4: s(TP_{MIX}) + s(AT), that is, axes scores are smooth functions of TP_{MIX} and AT.

m5: period + s(TP_{MIX}, by period), that is, axes scores are smooth functions of TP_{MIX} which differ between eutrophication and recovery periods.

m6: period + s(TP_{MIX}, by period) + AT, that is, axes scores are smooth functions of TP_{MIX} which differ between eutrophication and recovery periods, and are additionally influenced by AT.

m7: period + s(TP_{MIX}, by period) + s(AT), that is, axes scores are smooth functions of TP_{MIX} which differ between eutrophication and recovery periods, and are additionally smooth functions of AT.

m8: s(AT), that is, axes scores are smooth functions of AT.

The above models provide tests of the alternative hypotheses (a) no hysteresis in response to TP (m1), (b) hysteresis (m2, m5), (c) pseudo-hysteresis due to AT (m3, m4), (d) hysteresis and AT effects (m6, m7), and (e) solely AT effects (m8). Models were ranked according to AICc and Akaike weights. For all models, patterns in the residuals were examined. In addition, all models were run with and without autocorrelated errors. As models without autocorrelated errors (with the exception of m1) outperformed models that included autocorrelated errors, we report only models without autocorrelated errors.

To study uncertainty of dating, we run all 8 models 999 times, in which sediment layer ages ($n = 25$) were randomly selected—without replacement—from the years 1954–2010 ($n = 57$), whereby selected years were ordered to maintain a monotonically increasing sequence of ages. Only the start and end years (1954 and 2010) were kept in all runs, as those years could be identified with high certainty because they represent a flooding layer and the top of the sediment core, respectively. This randomization procedure is highly conservative as it allows for aging errors larger than has been estimated for our dating method (± 3 yr, Wessels et al. 1995). For all iterations we selected all best models according to AICc, that is, those models which differ less than 2 in AIC_C from the model with the lowest AICc (Burnham and Anderson 1998). In addition, we identified the truly best models for those randomization runs in which the best model differed by more than two from the 2nd best model. Hence, for each randomization run there could be several models among the best models, but only one or possibly no truly best model. Statistical analyses were performed using R version 3.5.1 (R_Core_Team 2018) with packages vegan (Oksanen et al. 2018), mgcv (Wood 2006), and segmented (Muggeo 2008).

Results

Total phosphorus concentrations during winter mixing (TP_{MIX}) show that in the early 1950s the lake was still oligotrophic (i.e., $TP_{MIX} < 10$ $\mu g\ L^{-1}$), and increased rapidly toward a maximum (87 $\mu g\ L^{-1}$) at the end of the 1970s. Thereafter, TP_{MIX} decreased and was back to values ≤ 10 $\mu g\ L^{-1}$ in the 2000s (Fig. 1b). Upper 20m summer averages (TP_{JAS}) show similar dynamics as TP_{MIX} albeit with considerably lower maxima during the eutrophic period and faster increase during

eutrophication. Annual averages of AT increased during the last 100 yr by roughly 2°C with highest AT occurring since the 1990s (Fig. 1c). TP_{JAS} concentrations showed CWH in respect to TP_{MIX} (Fig. 1d): TP_{JAS} was high relative to TP_{MIX} during eutrophication when sewage plants were not in operation, started to decline earlier compared to TP_{MIX} after the onset of sewage plants operation, and was low relative to TP_{MIX} during the recovery period. In the range of TP_{MIX} between 35 and 75 μg L^{-1}, TP_{JAS} was on average 5.7 μg L^{-1} higher during the eutrophication compared to the recovery period (Fig. 1d).

Diatoms in all layers of the core were composed mainly of planktonic taxa (Fig. 2). Time-constrained cluster analyses suggests four periods of diverging diatom communities. Samples from the 1st period (1918–1935) (33.5–29 cm depth) were dominated by *Cyclotella* species (up to 70% relative abundance), for example, *Cyclotella cyclopuncta*, *Cyclotella*

pseudocomensis, *Cyclotella comensis*, and *Cyclotella ocellata*. Relative abundance of other taxa, for example, *Fragilaria crotonensis* Kitton and *Asterionella formosa* Hassall, never exceeded 6% in those early years. *Cyclotella* species decreased around the 1930/1940s during the 2nd period (1939–1958) concomitantly with the increase of *F. crotonensis* and the appearance of *Diatoma tenuis* Agardh and *Tabellaria flocculosa* Kützing (29–21 cm depth), the latter obtaining a relative abundance > 50%. The 3rd time period (1960–1996) encompasses the period of strongly increasing and subsequently decreasing TP_{MIX} values, with increases of *A. formosa* as well as *Stephanodiscus* species (e.g., *Stephanodiscus minutulus* Round and *Stephanodiscus hantzschii* Grunow), and rapidly decreasing relative abundances of *T. flocculosa*, which relative abundance was below 1% or absent from 1963 until 1987. In the mid-1970s for the 1st time the eutrophic species *Cyclostephanos*
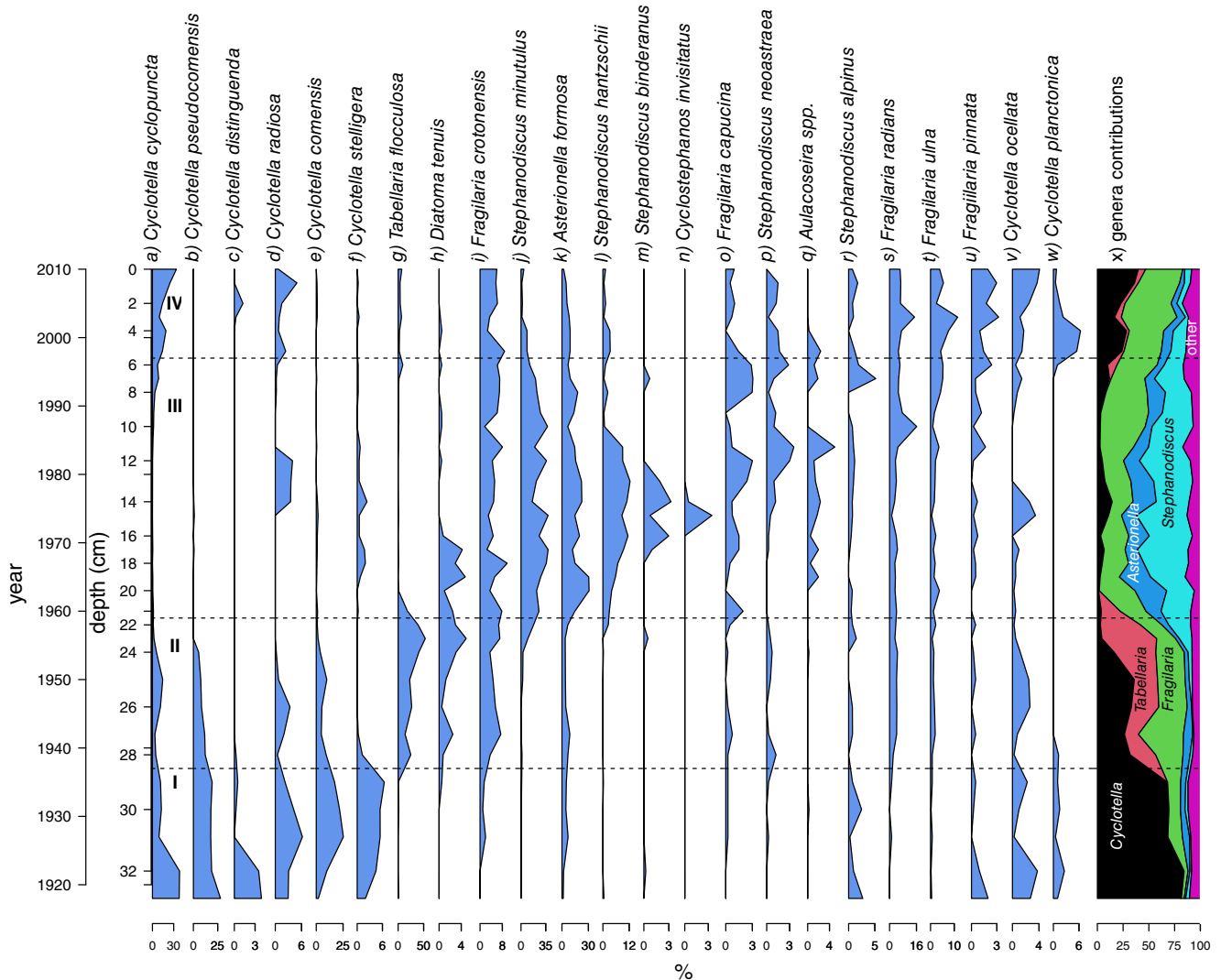

Fig. 2. Depth profile of the relative abundances of key diatom species (**a–w**) and of the contribution of genera *Cyclotella*, *Tabellaria*, *Fragilaria*, *Asterionella*, *Stephanodiscus*, and others to the total assemblage (*x*). Zones depicted (I–IV) are based on depth-constrained clustering.

invisitatus Theriot, Stoermer, and Håkasson appeared and *Stephanodiscus* species obtained relative abundances > 40%. From the late 1980s onwards, *Stephanodiscus* species started to decline and *Fragilaria* species achieved high relative abundances compared to previous years. The return of *Cyclotella* (*C. cyclopuncta*, *C. ocellata*, *C. radiosa* and *C. planctonica*) reaching relative abundances > 30% characterized the most recent layers (4th period, 1998–2010, 6–0 cm, Fig. 2), in which also *Stephanodiscus* species and most of the planktonic Fragilariaceae decreased (with the exception of *Fragilaria ulna* Lange-Bertalot and *Fragilaria pinnata* Ehrenberg). From the late-1980s onwards, *T. flocculosa* also increased, however, without reaching its dominance of the 1940/1950s.

Average-linkage clustering without considering time constraints suggests four time periods, which largely agree with those identified using time constrained clustering (Fig. 3a). In a 1st step, the years 1918–1935, that is, the most oligotrophic years were separated from the remaining years. In a 2nd step, the most eutrophic years 1960–1992 were separated from the oligo-mesotrophic periods 1939–1958 and 1994–2010. In a 3rd step, the oligo-mesotrophic period during eutrophication (1939–1958) was separated from the oligo-mesotrophic period that occurred during recovery (1994–2010). The two clustering methods differ only in grouping of the middle 1990s that were

still considered part of the eutrophic period in time-constrained clustering, but part of the 2nd mesotrophic period in average-linkage clustering.

The most oligotrophic years separated most strongly from all other years in a PCA biplot (Fig. 3b) considering all study years. The 1st axis explained 40.48% and separates the oligotrophic from the eutrophic years with highest absolute loadings for *Stephanodiscus minutulus* occurring mostly in eutrophic years and *Cyclotella cyclopuncta* and *C. pseudocomensis* occurring mostly in oligotrophic years. The 2nd axis explained 18.18% of the variation in diatom counts and separates samples with a high relative frequency of *T. flocculosa* from all other samples. The most recent years cluster together with the late 1930s until early 1950s. The 3rd PCA axis explained 12.29% of overall variability with axis scores linearly increasing with study year from the 1930 to recent years. TP_{MIX}, AT, and study year were correlated to 1st and 2nd axes scores (Fig. 3b). Vectors of AT and study year point in the same direction, with year showing a stronger relationship to PCA axes. The correlation of TP_{MIX} with the 2nd axis is inverse to the correlations of AT and year to the 2nd axis.

Scores of the 1st PCA axis (Fig. 4) closely follow the dynamics of log_{10}-transformed TP_{MIX} ($r = 0.78$, $t_{23} = 5.9$, $p < 0.0001$), that is, linear change along PCA1 is associated with
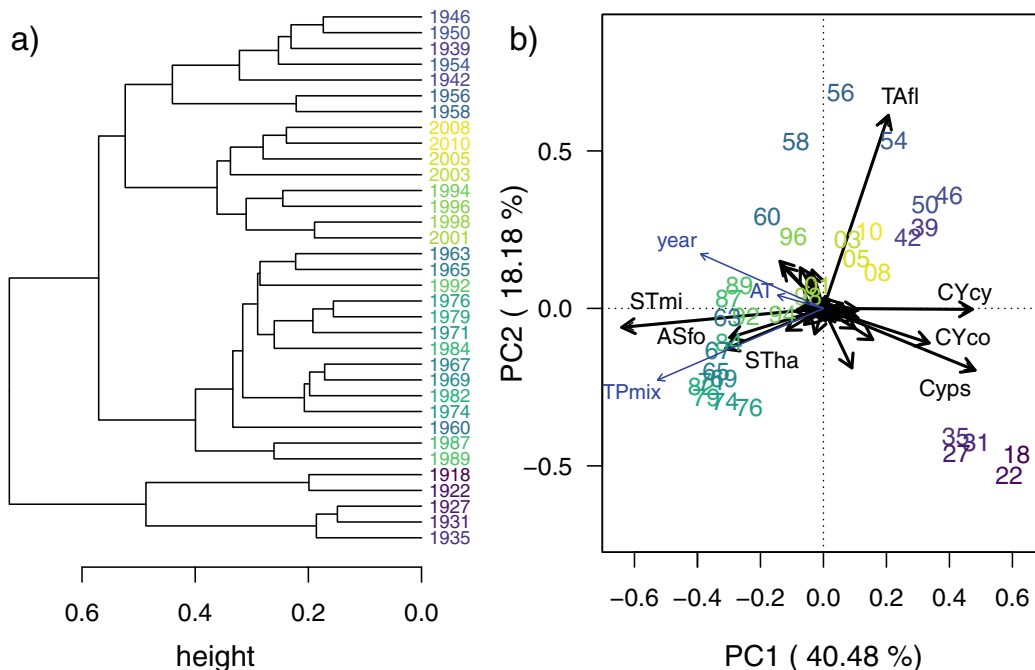

Fig. 3. (**a**) Dendrogram based on hierarchical average linkage cluster analysis, (**b**) PCA biplot for diatom community dynamics from 1918 to 2010. The color gradient is chronological ranging from dark purple (1920/1930s) via blue (1950s), bluegreen (1970s), lightgreen (1990s), and yellow (2000s). Years in the PCA biplot are shown as two-digit numbers. Species indicated are *Cyclotella stelligera* (Cyst), *Cyclotella comensis* (CYco), *Cyclotella pseudocomensis* (CYps), *Cyclotella cyclopuncta* (CYps), *Tabellaria flocculosa* (TAfl), *Asterionella formosa* (ASfo), *Stephanodiscus hantzschii* (STha), and *Stephanodiscus minitulus* (STmi). Blue arrows show the direction and strength of correlations between environmental variables and PCA scores of the 1st two axes. Significance of vectors based on a permutation test: TP_{MIX}: $p < 0.001$, AT: ns, year: $p < 0.0001$.
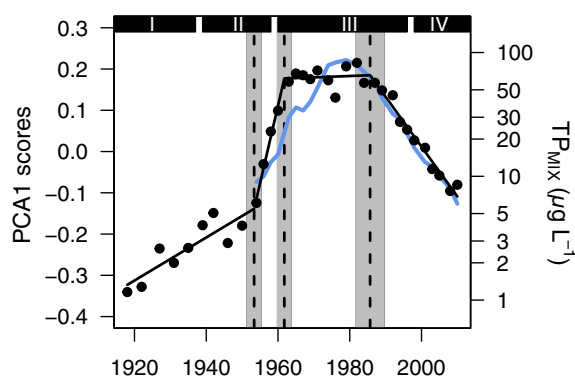
Fig. 4. Temporal development of the scores of the 1st PCA axis (dots) and measured TP_{MIX} (blue line). TP_{MIX} is shown on a log-transformed axis. Black lines represent the fit of a segmented regression model (Table 1) with breakpoints at 1953.3 ± 0.9, 1961.6 ± 0.9, 1985.5 ± 1.8 yr (gray rectangles). The black rectangles at the top of the graph show the diatom zonation revealed by time constrained clustering.

exponential dynamics of TP_{MIX}. However, relative to the change of TP_{MIX}, change of PCA axis 1 scores is faster during eutrophication as compared to the recovery period. Segmented regression of the 1st PCA axis identified four different periods of community change (Fig. 4, Table 1). A 1st period of slow change during the 1st part of the 20th century was followed by a decade of rapid change from 1951 until 1962. From 1962 until 1985 PCA1 scores did not change significantly, whereas thereafter, until the end of the investigation period, the rate of change was intermediate (Fig. 4; Table 1).

The 1st and 2nd axes scores showed a saturating relationship with TP_{MIX} with little change above a TP_{MIX} threshold of 30–40 μg L^{-1} especially during eutrophication. In contrast, during recovery, values of both axes started to decrease almost immediately with decreasing TP_{MIX} (Fig. 5). Hence, the responses were asymmetric and showed CWH in respect to the direction of trophic change. PCA1 scores of the 2000s returned back to the scores of the 1950s (Fig. 5a), whereas PCA2 trajectories during eutrophication and recovery crossed resulting in scores of the 2000s larger than those of the 1950s (Fig. 5b).

For all three PCA axes, all models receiving support (Akaike weights > 0.01) included TP_{MIX} trajectories differing between eutrophication and recovery and supporting hysteresis (models m5, m6, m7, Table 2). Model m5 that did not include an additional effect of AT received 10 and 2 times more

support according to Akaike weights relative to m6 or m7 for PCA axis 1, respectively PCA axes 2 and 3. Effects of AT in models m6 and m7 were only significant for PCA axis 2, but not for PCA axes 1 and 3 (Table 2).

The randomization approach strongly supported the ranking of models based on non-randomized layer ages (Table 2 and Fig. 6). Model m5 was most often selected as truly best model, that is, AICc was lower by 2 units as the 2nd best model, as well was most often among the best models, that is, AICc was less than 2 units higher compared to the best model. Models testing for pseudo-hysteresis (m3 and m4) or with s(AT) as sole predictor were never selected as truly best model for axes 1 and 3 scores, and hardly for axis 2 scores (1% m4). Likewise, these models were also in the minority of runs among the best models. Model m1 was selected in 8% of model runs as best model for PCA axis 1. However, in these models a temporal pattern in the residuals was still apparent.

Discussion

Diatom community change in Lake Constance was strongly influenced by an increase and subsequent decrease of phosphorus concentrations. We identified four periods of change: a period of slow community change until the early 1950s, a decade of rapid community change during the 1950s/early 1960s, $2^{1}/_{2}$ decades of rather stable community composition, and from the mid-1980s toward 2010 a reversal of community composition similar to the one observed in the early 1950s. Hence, the community shifted within one decade (1954–1962) from one still typical for oligotrophic conditions to one typical for eutrophic conditions, but returned to the former composition within a period of ~ 25 yr (1986–2010), that is, the diatom community trajectories relative to TP_{MIX} showed CWH dynamics.

These conclusions are unlikely affected by errors in dating of sediment layers as flood layers allowed for precise dating of individual events throughout the study period and dating of other layers via linear interpolation introduced a maximum error of ± 3 yr (Wessels et al. 1995). Our randomization approach of sediment layer dating, which allowed an even larger error as detected by Wessels et al. (1995) did also support our conclusions. Finally, dating accuracy is also supported via comparison of diatom remains with plankton counts (Auerbach et al. 1924; Grim 1939; Lehn 1969; Kümmerlin and Bürgi 1989; Sommer et al. 1993). For example, there is a remarkable accordance with the plankton time series available for *T. flocculosa*: according to Grim (1939), this species, identified as *T. fenestrata*, was not present in the lake in 1935, but dominated the pennate community in 1939. Sampling in the 2nd half of the 20th century revealed that *T. flocculosa* strongly declined in the early 1960s (Lehn 1969) and increased again only from the mid-1980s onwards (Kümmerlin 1998). Strikingly similar dynamics of this species is observed in the data based on diatom remains in the

Table 1. Changes in slopes of PCA1 scores vs. time resulting from a segmented regression model.

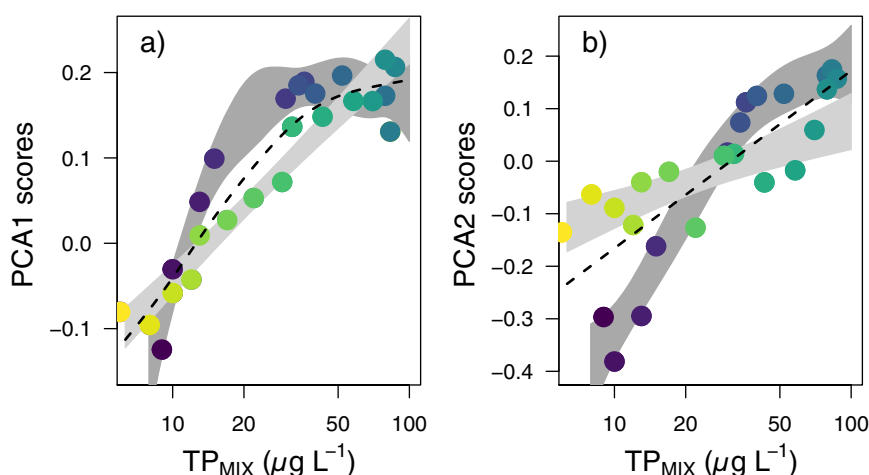|	Slope $\pm$ SE	95% CI	*t* value
1918–1953	0.0052 ± 0.0008	[0.0035, 0.0069]	6.26
1954–1962	0.0375 ± 0.0057	[0.0258, 0.0493]	6.54
1963–1985	0.0003 ± 0.0012	[−0.0021, 0.0028]	0.28
1986–2010	-0.0121 ± 0.0011	[−0.0143, −0.0099]	−11.38

Fig. 5. Relationships of (**a**) 1st and (**b**) 2nd PCA scores with TP_{MIX} during the period when TP_{MIX} values are available (1954–2010). The polygons show model m5 gam fits $\pm$ SE during the eutrophication period (until 1979, dark gray) and the oligotrophication period (from 1979 onwards, light gray). The dashed lines present gam fits of the relationships between the axes scores and TP_{MIX} for eutrophication and oligotrophication periods combined (models m1). The color gradient is chronological ranging from dark purple (1950/1960s) via bluegreen (1970/1980s), to yellow (2000s).

Table 2. Lists of the five best models predicting PCA axes 1–3 scores dynamics based on Akaike information criterion corrected for small sample size (AICc). The relative support for each of the models is given as model weight. Factors and smooth functions written in bold were significant at $p < 0.05$. *See* "Materials and methods" section for a description of all eight models compared.

PCA axis 1

Model	df	dAICc	Weight
m5: **Period** + **s(TP$_{MIX}$, by = period)**	7.9	0	0.847
m6: **Period** + **s(TP$_{MIX}$, by = period)** + AT	8.8	4.8	0.08
m7: **Period** + **s(TP$_{MIX}$, by = period)** + s(AT)	8.8	4.8	0.08
m2: **Period** + **s(TP$_{MIX}$)**	6.6	17.8	<0.0001
m1: **s(TP$_{MIX}$)**	5.2	17.9	<0.0001

PCA axis 2

Model	df	dAICc	Weight
m5: Period + **s(TP$_{MIX}$, by = period)**	7	0	0.48
m6: Period + **s(TP$_{MIX}$, by = period)** + AT	8.4	1.2	0.26
m7: Period + **s(TP$_{MIX}$, by = period)** + s(AT)	8.4	1.2	0.26
m4: **s(TP$_{MIX}$)** + s(AT)	4	24.3	<0.001
m3: **s(TP$_{MIX}$)** + AT	4	24.3	<0.001

PCA axis 3

Model	Df	dAICc	Weight
m5: **Period** + **s(TP$_{MIX}$, by = period)**	5	0	0.57
m7: **Period** + **s(TP$_{MIX}$, by = period)** + s(AT)	6	2.0	0.21
m6: **Period** + **s(TP$_{MIX}$, by = period)** + AT	6	2.0	0.21
m2: **Period** + **s(TP$_{MIX}$)**	4	37.9	<0.001
m3: **s(TP$_{MIX}$)** + **AT**	4	37.9	<0.001

Note: Factors and smooth functions written in bold were significant at $p < 0.05$.

sediment core, for example, low relative abundances (< 0.1%) in 1935, high relative abundance in 1939 (~ 25%) and thereafter, strong decline during the early 1960s and slow increase from the late-1980s onwards.

We used three different methods to group sediment layers: segmented regression of PCA1 scores and two clustering methods. The clustering methods provided rather similar results, considered all diatom taxa, but provided a rather static view of diatom dynamics. In contrast, grouping of years identified by segmented regression was based on 40% of diatom variability represented by the 1st PCA axis, but allowed a rather dynamic view of changes which occurred also within the groups of years identified by cluster analyses. This approach suggests that the diatom community neither at the start nor at the end of the time series was in a stable state, and allows a quantification of the rate of change during various periods of community dynamics.

Based on the segmented regression results, we identified four periods of community change: slow community and rapid community response to eutrophication, community stability above a threshold of 30–40 μg TP L^{-1}, and community response during recovery. These periods are supported by various independent time series: Changes in the 1st half of the last century are not well documented, but an increase in fishery yield during this period (Eckmann and Rösch 1998) suggests increases in lake productivity. In contrast, the rapid changes occurring during the 1950s are documented for several food web components (Lehn 1969; Walz et al. 1987). Likewise, the community changes observed during early eutrophication, that is, before the 1950s, and accelerated eutrophication, for example, the decline of *Cyclotella* species, increases of *A. formosa*, *Stephanodiscus* species and *Aulacoseira* spp. agree
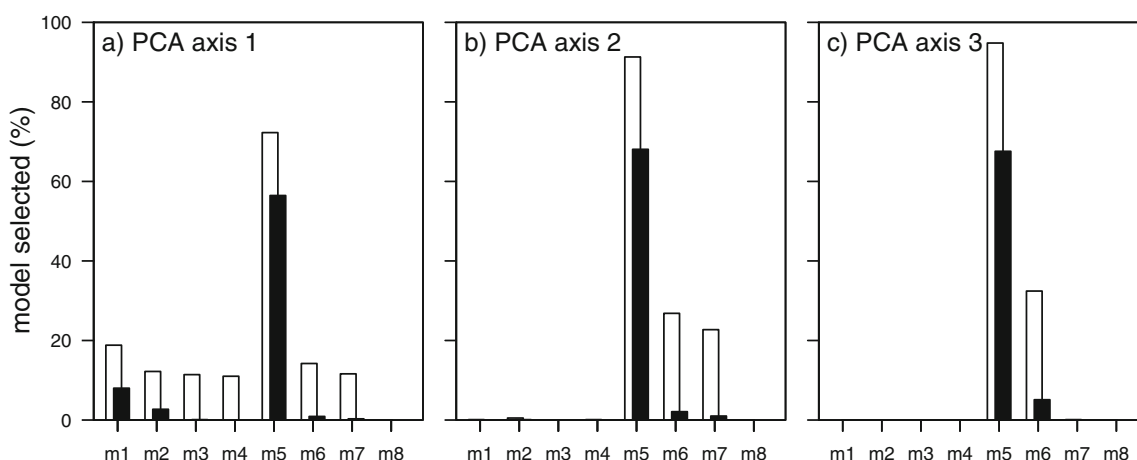
Fig. 6. Models selected among the best models (white bars) and as truly best models (black bars) in 999 model runs for each axis with randomized sequences of estimated sediment layer ages. For model descriptions, *see* "Materials and methods" section. Model m1 suggests no hysteresis, models m2 and m5 support CWH, models m3 and m4 pseudo-hysteresis due to AT, models m6 and m7 suggest CWH and additionally a role of AT, whereas m8 suggests AT as only driver of diatom dynamics.

well with a previous study of Lake Constance diatoms (Wessels et al. 1999), and with studies on other peri-alpine lakes (Alefs and Müller 1999; Marchetto et al. 2004; Bigler et al. 2007; Thies et al. 2012; Berthon et al. 2014; Milan et al. 2015). The finding of rather stable community composition during 1962–1985 is supported from long-term data of phytoplankton, which showed constant annual average phytoplankton biomasses from 1965 to 1990, that is, above a TP_{MIX} threshold of 30–40 μg L^{-1} (Jochimsen et al. 2013).

The diatom community showed a large degree of reversibility based on PCA and cluster analyses. The degree of reversibility should be judged by a comparison of most recent years with those of the early 1950s, as current TP_{MIX} concentrations are similar to those of the 1950s, but likely higher than those of the 1920s (Straile 2015). Hence, if we assume phosphorus to be the dominant driver of diatom community composition, we cannot expect that diatoms will return to the community composition of the 1920s, but only to those of the 1950s. PCA axis 1 scores of the 2000s indeed returned to values, which were typical for the early 1950s. In addition, cluster analysis—when dividing all years into three distinct groups—suggests one cluster combining all oligo-mesotrophic years independently whether this trophic status occurred during eutrophication or during recovery. This is supported by plankton measurements showing that diatom species which declined below detection level during eutrophication were found again with recovery, and vice versa, species rising above detection level with eutrophication disappeared again, or at least strongly decreased in relative abundance (Kümmerlin 1998). Such a high degree of reversibility was not observed in a set of 12 lakes studied by Bennion et al. (2015). Only in their two deepest lakes (Lake Bled, Slovenia, and Lake Mjøsa, Norway) a significant reversal toward the pre-eutrophication flora was observed, whereas for more shallow lakes results were unclear.

Likewise, in two deep peri-alpine French lakes, Lake Bourget and Lake Geneva, a rather high degree of reversibility was observed (Berthon et al. 2014). As in Lake Constance, also in these lakes PCA1 scores explained roughly 40–50% of diatom variability, and in recent years closely approached the scores of the 1950s (Berthon et al. 2014). Hence, our data support results from other deep lakes showing that diatom community composition may show considerable recovery.

However, in addition to previous studies, our data show different trajectories during eutrophication vs. recovery, that is, at similar TP_{MIX}, diatom community status differed between the eutrophication and recovery periods. Our GAM results suggest that this hysteresis is unlikely explained by a temperature increase (pseudo-hysteresis), but more likely a direct response to eutrophication and recovery (true CWH). Air and water temperatures increased most strongly during the late 1980s (Jochimsen et al. 2013), that is, during the recovery period. This suggests that AT should also contribute significantly to models examining only this period. However, when running a PCA only for the recovery period, there was only one significant axis according to the broken stick model, and axis dynamics were strongly related to TP_{MIX} without any evidence for a role of AT (analyses not shown). Therefore, AT potentially only played a (weak) role in models when both the eutrophication and recovery periods were considered in statistical analysis, that is, only if there was a possibility that hysteretic dynamics might be erroneously attributed to warming effects.

CWH is further supported by the dynamics of epilimnetic TP_{JAS} concentrations that also were higher during eutrophication compared to recovery. Such differences might be expected given that during the eutrophication period, there was hardly any P elimination in sewage plants in the catchment of Lake Constance in operation. Although 1st sewage

plants were built in the 1960s, it took until 1972 until 24% of the wastewater was treated with phosphorus elimination (Mürle et al. 2004). Thereafter, phosphorus elimination in sewage plants rose rapidly to 88% in 1985 and 97% in 2001 (Mürle et al. 2004). That is, during eutrophication, a large amount of phosphorus was entering the lake close to the surface, throughout the year, and was immediately available for boosting phytoplankton production in the epilimnion. While this inflow also contributed to an increase of TP_{MIX}, the increase of TP_{MIX} occurred more slowly because of the much larger volume of the overall water body compared to the epilimnion. In contrast, during the recovery period, the year-round supply of phosphorus into upper water layers and thus productivity was strongly reduced thereby likely also affecting epilimnetic producers rather immediately and more rapidly compared to whole water column phosphorus concentrations, that is, TP_{MIX}. However, as during early recovery TP_{MIX} was still high, epilimnetic productivity drew strongly from phosphorus supplied during winter mixing period. Hence, the reduction of the year-round phosphorus supply during the recovery period increased the relative importance of winter mixing for the annual phosphorus supply, and likely explains the close association of TP_{MIX} with PCA axis 1 dynamics during the recovery period (Fig. 4).

Hysteretic dynamics in response to phosphorus changes are also evident in studies analyzing growth rates (Thomas and Eckmann 2007) and stable isotope signatures (Gerdeaux and Perga 2006) of whitefish (*Coregonus wartmanni*), the dominant planktivorous fish in Lake Constance. Slower whitefish growth at similar TP_{MIX} during recovery vs. eutrophication were suggested to be due to density dependent growth and fishery-induced evolution (Thomas and Eckmann 2007). More negative $\delta^{13}C$ signatures at similar annual average TP concentrations during recovery vs. eutrophication were suggested to be due to climate warming (Gerdeaux and Perga 2006). That is, according to the results in these studies and the definitions used in this paper, the observed patterns were pseudo-hysteretic. However, a lower TP_{MIX} specific productivity during recovery vs. eutrophication (*see* above) indeed predicts lower TP_{MIX} specific whitefish growth rates and less negative TP_{MIX} specific $\delta^{13}C$ values during recovery vs. eutrophication. Hence, the patterns presented in the two whitefish studies can be explained more parsimoniously without the need of additional drivers (e.g., warming or fishery-induced evolution), and thus support the presence of true CWH. Unfortunately, as the CWH hypothesis for deep lakes is novel and thus could not be considered ~ 15 yr ago, Gerdeaux and Perga (2006) and Thomas and Eckmann (2007) did not test explicitly between these two alternative hypotheses, that is, true CWH vs. pseudo-hysteretic dynamics due to warming or fishery induced evolution.

The dynamics of the 2nd PCA axis was primarily driven by *T. flocculosa*, which relative abundances decreased after 1954, strongly declined in the 1960s, and finally increased after the

mid-1980s. The decline after the 1950s and later increase relative to TP_{MIX} was initially also CWH (Fig. 5b). However, relative abundances of *T. flocculosa* during recovery did not reach similar relative abundances as those in the 1950s resulting in a crossing of eutrophication and recovery trajectories for PCA axis 2. AT contributed significantly to the 2nd best model (m6) explaining PCA2 scores, which might suggest that the increase of AT contributed to the reduced relative abundance with recovery. However, an opposite pattern was observed in Lake Mjøsa, Norway, in which relative abundances of *T. flocculosa* with recovery were higher than those observed with early eutrophication, a difference which was suggested to be due to warming (Hobaek et al. 2012). This shows that more work is needed to establish a thorough understanding of temperature effects on diatom dynamics. However, *Tabellaria* dynamics might also result from competition between diatom species and priority effects (Young et al. 2001). For example, experimental work showed that *Tabellaria fenestrata*, a close relative of *T. flocculosa*, was not able to invade *F. crotonensis* cultures under phosphate limited conditions, but vice versa (Tilman and Sterner 1984). This might suggest that *T. flocculosa* was not be able to increase abundances in the presence of competitively superior taxa under recovery conditions of low phosphorus supply, but during the high and unimpeded phosphorus supply into the euphotic zone prior to the establishments of sewage plants. Hence, differences in phosphorus supply in combination with priority effects might also drive differences in trajectories between the eutrophication and recovery periods.

Although we did not find strong evidence for effects of warming on diatom dynamics, this does not imply that warming had no influence on Lake Constance ecosystem dynamics. In contrast, climate change and variability have been shown to affect water column temperatures (Straile et al. 2003, 2010; Fink et al. 2014) and plankton phenologies (Straile 2000; Peeters et al. 2007; Seebens et al. 2007; Straile et al. 2015). Changes in water temperatures from 1965 toward the end of our study period were best described as a stepwise increase at the end of the 1980s (Jochimsen et al. 2013), separating years with rather stable annual average temperature before and after this stepwise increase. Biomass of various phytoplankton groups, including diatoms, has been found to be strongly influenced by phosphorus concentrations; however, no influence of water temperature change was detected (Jochimsen et al. 2013), which supports the results of this study. Hence, analyses of long-term data suggest strong phenological responses, but no annual mean responses of plankton to warming in Lake Constance. As the sediment record will preliminary report abundances averaged across several years, the absence of a strong climatic signal in the sedimentary record does not contradict the observed phenological responses to climate variability in long-term time series. Nevertheless, we cannot exclude that warming contributed also to the sedimentary diatom dynamics as weights for models

including AT as a predictor reached up to 10% for axis 1, 26% for axis 2, and 21% for axis 3. However, models not including a role of AT received substantially more support suggesting that true CWH is a previously overlooked pattern for the response of deep lakes to increases and declines of nutrients.

To conclude, our study shows CWH of diatom community structure and of epilimnetic summer TP relative to TP_{MIX}. The latter suggests that the diatom CWH is a response to changes in one stressor, that is, phosphorus, mediated by the differences in the distribution of phosphorus within the water column between eutrophication and recovery. In contrast, our analyses found only week support for the alternative hypothesis that warming contributed significantly to the observed hysteresis, that is, for pseudo-hysteretic dynamics. Future studies analyzing eutrophication and recovery in deep lakes should consider CWH as a hypothesis to explain differences between eutrophication and recovery trajectories.

Data availability statement

Data presented in this study are available within the PANGEA repository at https://www.pangaea.de.

References

Alefs, J., and J. Müller. 1999. Differences in the eutrophication dynamics of Ammersee and Starnberger See (Southern Germany), reflected by the diatom succession in varve-dated sediments. J. Paleolimnol. **21**: 395–407. doi:10.1023/A:1008098118867

Auer, I., R. Böhm, A. Jurkovic, and others. 2007. HISTALP—Historical instrumental climatological surface time series of the Greater Alpine Region. Int. J. Climatol. **27**: 17–46. doi:10.1002/joc.1377, 1

Auerbach, M., W. Maerker, and J. Schmalz. 1924. Hydrographisch-biologische Bodensee-Untersuchungen. I. Ergebnisse der Jahre 1920–1922. Arch. Hydrobiol. Suppl. **3**: 597–738.

Battarbee, R. W., V. J. Jones, R. J. Flower, N. G. Cameron, H. Bennion, L. Carvalho, and S. Juggins. 2001. Diatoms, p. 155–202. *In* J. P. Smol, H. J. B. Birks, and W. M. Last [eds.], Tracking environmental change using Lake sediments. Volume 3: Terrestrial, algal, and siliceous indicators. Kluwer Academic Publishers.

Battarbee, R. W., N. J. Anderson, H. Bennion, and G. L. Simpson. 2012. Combining limnological and palaeolimnological data to disentangle the effects of nutrient pollution and climate change on lake ecosystems: Problems and potential. Freshw. Biol. **57**: 2091–2106. doi:10.1111/j.1365-2427.2012.02860.x

Bennion, H., J. Fluin, and G. L. Simpson. 2004. Assessing eutrophication and reference conditions for Scottish freshwater lochs using subfossil diatoms. J. Appl. Ecol. **41**: 124–138.

Bennion, H., and G. L. Simpson. 2011. The use of diatom records to establish reference conditions for UKlakes subject to eutrophication. J. Paleolimnol. **45**: 469–488. doi:10.1007/s10933-010-9422-8

Bennion, H., R. W. Battarbee, C. D. Sayer, G. L. Simpson, and T. A. Davidson. 2011. Defining reference conditions and restoration targets for lake ecosystems using palaeolimnology: A synthesis. J. Paleolimnol. **45**: 533–544. doi:10.1007/s10933-010-9419-3

Bennion, H., G. L. Simpson, and B. J. Goldsmith. 2015. Assessing degradation and recovery pathways in lakes impacted by eutrophication using the sediment record. Front. Ecol. Evol. **3**: 94. doi:10.3389/fevo.2015.00094

Berthon, V., B. Alric, F. Rimet, and M. E. Perga. 2014. Sensitivity and responses of diatoms to climate warming in lakes heavily influenced by humans. Freshw. Biol. **59**: 1755–1767. doi:10.1111/fwb.12380

Bigler, C., L. von Gunten, A. F. Lotter, S. Hausmann, A. Blass, C. Ohlendorf, and M. Sturm. 2007. Quantifying human-induced eutrophication in Swiss mountain lakes since AD 1800 using diatoms. Holocene **17**: 1141–1154.

Bollhöfer, A., A. Mangini, A. Lenhard, M. Wessels, F. Giovanoli, and B. Schwarz. 1994. High resolution ^{210}Pb-dating of Lake Constance sediments: Stable lead in Lake Constance. Environ. Geol. **24**: 267–274.

Bührer, H., P. Kirner, and G. Wagner. 2000. Dem Bodensee in den Abflussjahren 1996 und 1997 zugeführte Stofffrachten. Ber. Int. Gewässerschutzkomm. Bodensee **53**: 1–43.

Burnham, K. P., and D. R. Anderson. 1998. Model selection and inference—A practical information-theoretic approach. Springer.

Carpenter, S. R., and K. L. Cottingham. 1997. Resilience and restoration of lakes. Ecol. Soc. **1**:2. doi:10.5751/ES-00020-010102

Carpenter, S. R., D. Ludwig, and W. A. Brock. 1999. Management of eutrophication for lakes subject to potentially irreversible change. Ecol. Appl. **9**: 751–771 doi:10.1890/1051-0761(1999)009[0751:MOEFLS]2.0.CO;2.

Dodds, W. K., W. W. Bouska, J. L. Eitzmann, T. J. Pilger, K. L. Pitts, A. J. Riley, J. T. Schloesser, and D. J. Thornbrugh. 2009. Eutrophication of U.S. freshwaters: Analysis of potential economic damages. Environ. Sci. Technol. **43**: 12–19.

Dove, A., and S. C. Chapra. 2015. Long-term trends of nutrients and trophic response variables for the Great Lakes. Limnol. Oceanogr. **60**: 696–721. doi:10.1002/lno.10055

Duarte, C. M., D. J. Conley, J. Carstensen, and M. Sanchez-Camacho. 2009. Return to Neverland: Shifting baselines affect eutrophication restoration targets. Estuaries and Coasts **32**: 29–36.

Dubois, N., and others. 2018. First human impacts and responses of aquatic systems: A review of palaeolimnological records from around the world. Anthropocene Rev. **5**: 28–68. doi:10.1177/2053019617740365

Eckmann, R., and R. Rösch. 1998. Lake Constance fisheries and fish ecology. Arch. Hydrobiol. Spec. Issues Adv. Limnol. **53**: 285–301.

Fink, G., M. Schmid, B. Wahl, T. Wolf, and A. Wüest. 2014. Heat flux modifications related to climate-induced warming of large European lakes. Water Resour. Res. **50**: 2072–2085. doi:10.1002/2013WR014448

Gerdeaux, D., and M. E. Perga. 2006. Changes in whitefish scales δ13C during eutrophication and reoligotrophication of subalpine lakes. Limnol. Oceanogr. **51**: 772–780.

Grim, J. 1939. Beobachtungen am Phytoplankton des Bodensees (Obersee) sowie deren rechnerische Auswertung. Int. Rev. Gesamten. Hydrobiol. **39**: 193–315.

Güde, H., H. Rossknecht, and G. Wagner. 1998. Anthropogenic impacts on the trophic state of Lake Constance during the 20th century. Arch. Hydrobiol. Spec. Issues Adv. Limnol. **53**: 85–108.

Güde, H., and D. Straile. 2016. Bodensee—Ökologie und anthropogene Belastungen eines tiefen Voralpensees. Limnol. Aktuell **15**: 1–271.

Håkansson, H. 2002. A compilation and evaluation of species in the general *Stephanodiscus*, *Cyclostephanus*, and *Cyclotella* with a new genus in the family Stephanodiscaceae. Diatom Res. **17**: 1–139. doi:10.1080/0269249X.2002.9705534

Hobaek, A., J. E. Løvik, T. Rohrlack, S. J. Moe, M. Grung, H. Bennion, G. Clarke, and G. T. Piliposyan. 2012. Eutrophication, recovery and temperature in Lake Mjøsa: Detecting trends with monitoring data and sediment records. Freshw. Biol. **57**: 1998–2014. doi:10.1111/j.1365-2427.2012.02832.x

Houk, V., R. Klee, and H. Tanaka. 2010. Atlas of freshwater centric diatoms with a brief key and descriptions. Part III. Stephanodiscaceae A. Cyclotella, Tertiarius, Discostella. Fottea **10**: 1–498.

Ibelings, B. W., R. Portielje, E. H. H. R. Lammens, R. Noordhuis, M. S. van den Berg, W. Joosse, and M. L. Meijer. 2007. Resilience of alternative stable states during the recovery of shallow lakes from eutrophication: Lake Veluwe as a case study. Ecosystems **10**: 4–16.

Ibrahim, A., E. Capo, M. Wessels, I. Martin, A. Meyer, D. Schleheck, and L. S. Epp. 2021. Anthropogenic impact on the historical phytoplankton community of Lake Constance reconstructed by multimarker analysis of sediment-core environmental DNA. Mol. Ecol. **30**: 3040–3056. doi:10.1111/mec.15696

Jassby, A. D. 1998. Interannual variability at three inland water sites: Implications for sentinel ecosystems. Ecol. Appl. **8**: 277–287.

Jenny, J.-P., P. Francus, A. Normandeau, F. Lapointe, M. E. Perga, A. E. K. Ojala, A. Schimmelmann, and B. Zolitschka. 2016. Global spread of hypoxia in freshwater ecosystems during the last three centuries is caused by rising local human pressure. Glob. Chang. Biol. **22**: 1481–1489. doi:10.1111/gcb.13193

Jeppesen, E., and others. 2005. Lake responses to reduced nutrient loading - an analysis of contemporary long-term data from 35 case studies. Freshw. Biol. **50**: 1747–1771. doi:10.1111/j.1365-2427.2005.01415.x

Jochimsen, M. C., R. Kümmerlin, and D. Straile. 2013. Compensatory dynamics and the stability of phytoplankton biomass during four decades of eutrophication and oligotrophication. Ecol. Lett. **16**: 81–99. doi:10.1111/ele.12018

Krammer, K., and H. Lange-Bertalot. 1986. Die Süsswasserflora von Mitteleuropa 2: Bacillariophyceae. 1 Teil: Naviculaceae. Gustav-Fischer Verlag.

Kümmerlin, R. E. 1998. Taxonomical response of the phytoplankton community of Upper Lake Constance (Bodensee-Obersee) to eutrophication and re-oligotrophication. Arch. Hydrobiol. Spec. Issues Adv. Limnol. **53**: 109–117.

Kümmerlin, R., and H. R. Bürgi. 1989. Die langjährige Entwicklung des Phytoplanktons im Bodensee (1961-1986). Ber. Int. Gewässerschutzkomm. Bodensee **39**: 1–175.

Legendre, P., and E. D. Gallagher. 2001. Ecologically meaningful transformations for ordination of species data. Oecologia **129**: 271–280. doi:10.1007/s004420100716

Lehn, H. 1969. Die Veränderungen des Phytoplanktonbestandes im Bodensee I. Fluktuationen von Tabellaria fenestrata 1890–1967. Int. Rev. Gesamten. Hydrobiol. Hydrogr. **54**: 367–411. doi:10.1002/iroh.19690540304

Marchetto, A., A. Lami, S. Musazzi, J. Massaferro, L. Langone, and P. Guilizzoni. 2004. Lake Maggiore (N. Italy) trophic history: Fossil diatom, plant pigments, and chironomids, and comparison with long-term limnological data. Quat. Int. **113**: 97–110. doi:10.1016/S1040-6182(03)00082-X

Milan, M., C. Bigler, N. Salmaso, G. Guella, and M. Tolotti. 2015. Multiproxy reconstruction of a large and deep subalpine lake's ecological history since the Middle Ages. J. Great Lakes Res. **41**: 982–994. doi:10.1016/j.jglr.2015.08.008

Muggeo, V. M. R. 2008. Segmented: An R package to fit regression models with broken-line. R News **8**: 20–25.

Mürle, U., J. Ortlepp, and P. Rey. 2004. Der Bodensee, Zustand-Fakten-Perspektiven. Int. Gewässerschutzkomm. Bodensee.3-902290-04-8

Oksanen, J., and others. 2018. vegan: Community Ecology Package. R package version 2.5-3. https://CRAN.R-project.org/package=vegan

Peeters, F., D. Straile, A. Lorke, and D. M. Livingstone. 2007. Earlier onset of the spring phytoplankton bloom in lakes of the temperate zone in a warmer climate. Glob. Chang. Biol. **13**: 1898–1909. doi:10.1111/j.1365-2486.2007.01412.x

Pretty, J. N., C. F. Mason, D. B. Nedwell, R. E. Hine, S. Leaf, and R. Dils. 2003. Environmental costs of freshwater eutrophication in England and Wales. Environ. Sci. Technol. **37**: 201–208. doi:10.1021/es020793k

R_Core_Team. 2018. R: A language and environment for statistical computing, Vienna Austria. https://www.R-project.org/.

Salmaso, N., G. Morabito, L. Garibaldi, and R. Mosello. 2007. Trophic development of the deep lakes south of the Alps: A comparative analysis. Fund. Appl. Limnol. **170**: 177–196. doi:10.1127/1863-9135/2007/0170-0177

Scheffer, M., S. H. Hosper, M. L. Meijer, B. Moss, and E. Jeppesen. 1993. Alternative equilibria in shallow lakes. Trends Ecol. Evol. **8**: 275–279.

Schindler, D. W., and J. R. Vallentyne. 2008. The algal bowl: Overfertilization of the world's freshwaters and estuaries. Univ. Alberta Press.

Schmidt, R., C. Kamenik, H. Lange-Bertalot, and R. Klee. 2004. *Fragilaria* and *Staurosira* (Bacillariophyceae) from sediment surfaces of 40 lakes in the Austrian Alps in relation to environmental variables, and their potential for palaeoclimatology. J. Limnol. **63**: 171–189. doi:10.4081/jlimnol.2004.171

Seebens, H., D. Straile, R. Hoegg, H. B. Stich, and U. Einsle. 2007. Population dynamics of a freshwater calanoid copepod: Complex responses to changes in trophic status and climate variability. Limnol. Oceanogr. **52**: 2364–2372. doi:10.4319/lo.2007.52.6.2364

Sommer, U., U. Gaedke, and A. Schweizer. 1993. The first decade of oligotrophication of lake Constance. II. The response of phytoplankton taxonomic composition. Oecologia **93**: 276–284.

Steffen, W., W. Broadgate, L. Deutsch, O. Gaffney, and C. Ludwig. 2015. The trajectory of the Anthropocene: The Great Acceleration. Anthropocene Rev. **2**: 81–98. doi:10.1177/2053019614564785

Straile, D. 2000. Meteorological forcing of plankton dynamics in a large and deep continental European lake. Oecologia **122**: 44–50. doi:10.1007/PL00008834

Straile, D. 2015. Zooplankton biomass dynamics in oligotrophic versus eutrophic conditions: A test of the PEG model. Freshw. Biol. **60**: 174–183. doi:10.1111/fwb.12484

Straile, D., K. D. Jöhnk, and H. Rossknecht. 2003. Complex effects of winter warming on the physicochemical characteristics of a deep lake. Limnol. Oceanogr. **48**: 1432–1438.

Straile, D., O. Kerimoglu, F. Peeters, M. C. Jochimsen, R. Kümmerlin, K. Rinke, and K. O. Rothhaupt. 2010. Effects of a half a millennium winter on a deep lake—A shape of things to come? Glob. Chang. Biol. **16**: 2844–2856. doi:10.1111/j.1365-2486.2009.02158.x

Straile, D., O. Kerimoglu, and F. Peeters. 2015. Trophic mismatch requires seasonal heterogeneity of warming. Ecology **96**: 2794–2805.

Taranu, Z. E., and others. 2015. Acceleration of cyanobacterial dominance in north temperate-subarctic lakes during the Anthropocene. Ecol. Lett. **18**: 375–384. doi:10.1111/ele.12420

Thies, H., M. Tolotti, U. Nickus, A. Lami, S. Musazzi, P. Guilizzoni, N. L. Rose, and H. Yang. 2012. Interactions of temperature and nutrient changes: Effects on phytoplankton in the Piburger See (Tyrol, Austria). Freshw. Biol. **57**: 2057–2075. doi:10.1111/j.1365-2427.2011.02661.x

Thomas, G., and R. Eckmann. 2007. The influence of eutrophication and population biomass on common whitefish (*Coregonus lavaretus*) growth—The Lake Constance example revisited. Can. J. Fish. Aquat. Sci. **64**: 402–410.

Tilman, D., and R. W. Sterner. 1984. Invasions of equilibria: Tests of resource competition using two species of algae. Oecologia **61**: 197–200. doi:10.1007/BF00396760

Tolotti, M., N. Dubois, M. Milan, M. E. Perga, D. Straile, and A. Lami. 2018. Large and deep perialpine lakes: A paleolimnological perspective for the advance of ecosystem science. Hydrobiologia **824**: 291–321. doi:10.1007/s10750-018-3677-x

Walz, N., H. J. Elster, and M. Mezger. 1987. The development of the rotifer community structure in Lake Constance during its eutrophication. Arch. Hydrobiol. Suppl. **74**: 452–487.

Wessels, M., A. Lenhard, F. Giovanoli, and A. Bollhöfer. 1995. High resolution time series of lead and zinc in sediments of Lake Constance. Aquat. Sci. **57**: 291–304.

Wessels, M., K. Mohaupt, R. Kümmerlin, and A. Lenhard. 1999. Reconstructing past eutrophication trends from diatoms and biogenic silica in the sediment and the pelagic one of Lake Constance. J. Paleolimnol. **21**: 171–192.

Wood, S. N. 2006. Generalized additive models: An introduction with R. Chapman & Hall/CRC.

Young, T. P., J. M. Chase, and R. T. Huddleston. 2001. Community Succession and Assembly: Comparing, Contrasting and Combining Paradigms in the Context of Ecological Restoration. Ecological Restoration **19**: 5–18. https://doi.org/10.3368/er.19.1.5

Acknowledgments

Conflict of Interest

None declared.